Available online at www.sciencedirect.com
SCIENCE DIRECT®
International Journal of Pharmaceutics 293 (2005) 281–290
international journal of pharmaceutics
www.elsevier.com/locate/ijpharm

Pharmaceutical Nanotechnology

Pharmacokinetics and biodistribution of RGD-targeted doxorubicin-loaded nanoparticles in tumor-bearing mice

David C. Bibby [a,*], James E. Talmadge [b], Milind K. Dalal [a], Scott G. Kurz [b], Kevin M. Chytil [b], Stephen E. Barry [a], David G. Shand [a], Matthias Steiert [a]

[a] *Alnis BioSciences Inc., 5764 Shellmound St., Emeryville, CA 94608, USA*
[b] *University of Nebraska Medical Center, Omaha, NE 68198, USA*

Received 21 September 2004; received in revised form 22 December 2004; accepted 22 December 2004

Abstract

We report the biodistribution and pharmacokinetics (PK) of a cyclic RGD-doxorubicin-nanoparticle (NP) formulation in tumor-bearing mice. The NP core was composed of inulin multi-methacrylate with a targeting peptide, cyclic RGD, covalently attached to the NPs via PEG-400. Seventy-two percent of the doxorubicin was attached to the NP matrix via an amide bond; 28% of doxorubicin was entrapped as unconjugated drug. The PK of total, unconjugated and metabolized doxorubicin was examined for 5 days following intravenous (i.v.) administration of the NP formulation (250 μg doxorubicin equiv.), revealing a bi-exponential fix with a terminal half-life of 5.99 h. In addition, the biodistribution studies revealed decreasing drug concentrations over time in the heart, lung, kidney and plasma and accumulating drug concentrations in the liver, spleen and tumor. The drug concentration in these latter tissues peaked between 24 and 48 h with the liver, spleen and tumor containing 56, 3.5 and 1.8% of the administered dose at $t = 48$ h, respectively. In contrast to all of the organs studied, the tumors contained high levels of a doxorubicin metabolite.

Keywords: Pharmacokinetics; Biodistribution; Nanoparticles; Doxorubicin; Mice

1. Introduction

Doxorubicin is an anthracycline, widely used in the treatment of breast and ovarian cancer (Devita et al., 1989; Martindale, 1996; Vermorken, 2003). However, dose-limiting toxicities occur with doxorubicin therapy and include myelosuppression and cardiotoxicity. Congestive heart failure is of particular concern, and is dosage cumulative such that no more than 550 mg/m^2 is recommended as a lifetime total dose (Von Hoff et al.,

Abbreviations: CiBA, cystine bisacrylamide; Cl-66, mammary tumor clone-66; IMMA, inulin multi-methacrylate; I.S., internal standard; LOD, limit of detection; NaA, sodium acrylate; NP, nanoparticles; PEG 400 DBA, poly(ethylene glycol) 400-dibromoacetate

* Corresponding author. Tel.: +1 510 420 3760; fax: +1 510 420 3761.
E-mail address: alnis@alnis.com (D.C. Bibby).

0378-5173/$ – see front matter © 2005 Published by Elsevier B.V.
doi:10.1016/j.ijpharm.2004.12.021

1979). Reformulation of doxorubicin has been undertaken to improve its pharmacokinetic (PK) and pharmacodynamic profile and minimize its toxicity. Liposomal formulations, including Myocet™ (Elan Pharmaceuticals) and Doxil® (Ortho BioTech) have been approved for clinical use and have similar efficacies and improved toxicity profiles as compared with doxorubicin (Harris et al., 2002). Additional formulations are also being developed to improve drug delivery, including the use of *N*-(2-hydroxypropyl)methacrylamide (HPMA)–doxorubicin conjugates (Duncan et al., 1998; Kovar et al., 2003; Ulbrich et al., 2003). These conjugates form a hydrogel in which doxorubicin is covalently linked to the water-soluble, biocompatible polymer HPMA via its ketone (forming a hydrazone bond) or amine site (forming an aconityl or amide bond). In addition, peptidic spacers, such as Gly–Phe–Leu–Gly and Gly–Gly, have also been incorporated in an effort to impart a pH-sensitive release profile. Polymeric micelles, most notably comprised of pluronics (polyether block copolymers), PEG-phospholipid and poly(ethyleneglycol)-poly(aminoacid) (PEG-PAA) block copolymers, have also been employed to deliver chemotherapeutics (Kwon, 2003). A formulation comprised of doxorubicin covalently attached to a poly(aspartic acid) backbone, and with additional doxorubicin molecules physically loaded into the core, has advanced to Phase II clinical trials in Japan (Kwon et al., 1994). In this formulation, only the physically entrapped doxorubicin molecules, and not covalently attached doxorubicin, are bioactive and tumorcidal.

The use of peptides capable of targeting tumor is one of the more recent developments for improving the performance and safety of selected chemotherapeutics. A number of RGD peptides and peptidomimetics have been shown to bind preferentially to particular integrins, for instance integrin αvβ3, which is often overexpressed on endothelial cells in tumor neovasculature (Pasqualini et al., 1997). Recently, anti-tumor efficacy was improved by targeting doxorubicin-loaded liposomes to the vasculature of colon cancer using RGD peptides in a xenograft mouse (Schiffelers et al., 2003). The targeting of integrin αvβ3 may lead to endocytosis of the doxorubicin-containing particles, subsequent killing of endothelial cells and tumor vasculature destruction.

We have developed carbohydrate-based NPs incorporating doxorubicin for the treatment of cancer. These NPs are typically between 15 and 30 nm in diameter with a core comprised of a modified, cross-linked carbohydrate: inulin multi-methacrylate (IMMA). Doxorubicin is covalently bound to the NP core via an amide bond. A targeting element consisting of a cyclic peptide with the RGD sequence: cyclo(–Arg–Gly–Asp–D–Phe–Cys–), is also attached using a PEG tether. We report herein our studies using these unique hydrophilic NPs with covalently attached doxorubicin. To define the PK and biodistribution of this formulation a murine mammary tumor model is described.

2. Materials and methods

2.1. Chemicals

Doxorubicin HCl, doxorubicinol and doxorubicinone were purchased from Qventas (Branford, CT). Daunorubicin HCl and sodium acrylate (NaA) were obtained from Sigma (St. Louis, MO). The cyclic RGD peptide was supplied by Peptisyntha (Torrance, CA). Inulin was purchased from Carbomer (San Diego, CA). Inulin multi-methacrylate (Mw 1750 approximately), cystine bisacrylamide (CiBA) and poly(ethylene glycol) 400-dibromoacetate (PEG 400 DBA) were prepared in-house. All other reagents were at least analytical reagent (AR) grade and solvents were high performance liquid chromatography (HPLC) grade.

2.2. Mice and tumors

Female Balb/cJ ($H2^d$) mice, 6 weeks of age, were purchased from Charles River (Wilmington, MA) and allowed to acclimate for 2 weeks prior to use. The mice were fed ad libitum and were maintained and handled under IACUC guidelines. The mammary fatpads of these mice were injected with the metastatic mammary tumor clone-66 (Cl-66; 300,000 tumor cells). The Cl-66 cell line was derived from a spontaneously arising Balb/cfC3H mouse mammary tumor in a Balb/cfC3H breeding female carrying mouse mammary tumor virus (Dexter et al., 1978). The cells were generously provided by Dr. Fred Miller of the Karamanos Cancer Center (Detroit, MI). This cell line has a high fre-

quency of experimental metastasis following i.v. injection and is known to spontaneously metastasize from primary tumors after injection into mammary fatpads or subcutaneous sites (Miller et al., 1983). Cl-66 was grown in Dulbecco's modified Eagle media with 10% fetal bovine serum (FBS) (HyClone, Logan, UT), 1% Pen/Strep, glutamine, pyruvate, essential and non-essential amino acids and 2% vitamins (Life Technologies, Gaithersburg, MD). The cells were briefly (2–3 min) trypsinized and washed twice with phosphate buffered saline (PBS), resuspended in PBS at 300,000 cells/0.1 mL and injected into the mammary fat pad (Talmadge et al., 1985). Mice ($n = 25$) were administered the test formulation 21 days following injection with Cl-66 and had a median tumor volume of $625 \pm 56\,mm^3$. Tumors were measured in two dimensions using digital calipers, and the volume calculated using the formula for a prolated sphere: $0.5 \times A \times B^2$, where A is the larger diameter and B is the smaller, perpendicular diameter.

2.3. Preparation of NPs

NPs were prepared via free radical polymerization in a water-in-oil "reverse" microemulsion. The dispersed aqueous phase of the reverse microemulsion (containing the building block materials) was comprised of 83:14:2:1 wt% water:IMMA:CiBA:NaA, and subsequently formed the cross-linked NP core. Cyclic RGD peptide was attached to the particle using a PEG linker (PEG 400 DBA). The NPs were prepared as a lyophilized powder, incorporating inulin as an excipient to aid in dissolution at an approximate weight ratio of 1:1 (NP:inulin). Doxorubicin was attached to carboxyl moieties on the particle (using 1-ethyl-3-dimethylaminopropyl) carbodiimide hydrochloride (EDC)) to form an amide bond.

2.4. Nanoparticle characterization

Total and unconjugated doxorubicin content was determined using the method of Seymour et al. (1990). Sample analysis (2–5 mg) was undertaken in triplicate. For the PK study, the total drug content of the prepared test article (including inulin) was determined to be $3.30 \pm 0.05\%$ (w/w); ca. 28% of the loaded drug ($0.93 \pm 0.01\%$, w/w) was encapsulated in an unconjugated state. RGD content was analyzed using a HCl hydrolysis technique at the HHMI/Keck Biotechnology Resource Laboratory, Yale University (New Haven, CT) and reported to be 34.8 μg/mg of NPs.

2.5. Pharmacokinetic and biodistribution study

Immediately prior to dosing, the test article was reconstituted in water at a concentration such that the dose would contain 250 μg doxorubicin (equiv.) in a 150 μL volume. Individual animal weights were recorded on the day of dosing. The mean ± S.D. weight for the animals at dosing ($n = 25$) was 18.96 ± 1.11 g. At each time point, blood was collected from five mice and centrifuged to separate the plasma. The plasma was divided into 2×50 μL aliquots (per time point, per mouse), individually placed into polypropylene Cryovials® (Spectrum Laboratories, New Brunswick, NJ) and immediately frozen at −80 °C. At selected times ($t = 0.25$, 6, 24, 48 and 120 h), a cohort of animals ($n = 5$) was sacrificed and the following tissues collected for analysis: heart, lung, spleen, liver, tumor and kidney. The cardiac tissue was sectioned and blotted with lint-free paper toweling to remove residual blood. No attempt was made to remove blood from other tissues. All tissues were labeled and placed into polypropylene Cryovials®, and immediately frozen at −80 °C until analysis. Plasma and tissues from non-dosed mice ($n = 18$) were also collected for the preparation of standard curves. PK parameters were calculated using Kinetica v4.2 (InnaPhase Corp., Philadelphia, PA); a standard i.v. bolus non-compartmental method was selected for the plasma PK.

2.6. HPLC analysis

The doxorubicin content in the NPs and the biological samples was determined by HPLC. The HPLC system consisted of a ProStar 210 solvent delivery module, equipped with a Prostar 363 fluorescence detector. Sample introduction was automated using a Prostar 410 autosampler (Varian Inc., Walnut Creek, CA). Chromatography was performed on a ChromSep HPLC glass column (100 mm × 3 mm) packed with Chromspher C8 (5 μm) stationary phase and equipped with a Chromsep guard column (Varian). Sample volumes of 50 μL were injected.

Mobile phase consisted of acidified water (pH 2.5; adjusted with TFA):acetonitrile:tetrahydrofuran

(80:35:1, v/v/v) and was delivered isocratically at a flow rate of 0.4 mL/min. Column eluent was monitored fluorometrically using an excitation wavelength of 460 nm and an emission wavelength of 550 nm (bandwidth = 30 nm). These chromatographic conditions were first reported by Van Asperen et al. (1998).

2.7. Preparation of standards

For the determination of both total (conjugated + unconjugated) and unconjugated doxorubicin, mouse plasma (50 μL) was spiked with doxorubicin to establish a standard curve. Standards were prepared in triplicate at six concentrations ranging from 50 to 10,000 ng of doxorubicin HCl. In addition, an internal standard (I.S.), daunorubicin-HCl (2500 ng), was added to each vial. Because of the potential for organ or tissue dependent interference of analysis, standard curves for each organ were also undertaken. These standards were prepared in triplicate at six concentrations ranging from 100 to 20,000 ng of added doxorubicin. Daunorubicin-HCl (5000 ng) and 1 mL of saline was also added to each vial. These preparations were then homogenized (approximately 30 s) with a hand-held homogenizer, the tissue homogenate divided equally and analyzed for total or unconjugated doxorubicin content.

Standard curves for plasma and each tissue type were prepared for both the total and unconjugated doxorubicin assays. In all cases, the function of analyte/I.S. peak area ratio versus doxorubicin concentration was linear over the range analyzed, though assay gradients varied depending on the tissue type. The retention times were: 4.3 min (doxorubicinone) and 8.1 min (daunorubicinone; I.S.) for the total drug assay, and 6.5 min (doxorubicin) and 12.1 min (daunorubicin; I.S.) for the unconjugated drug assay. These retention times were confirmed using commercially available compounds.

2.8. Determination of total doxorubicin content (degradation assay)

The method utilized was a modification of that reported by Seymour et al. (1990). Total doxorubicin content was determined by heating the sample under acidic conditions. This allowed cleavage of the glycosidic bond between the glycone and aglycone moiety of doxorubicin and the formation of doxorubicinone, which was subsequently extracted. To each standard or sample (containing I.S.), 0.5 mL of 1 M HCl was added and the vial heated at 80 °C for 20 min. An equal volume (0.5 mL) of Tris–HCl buffer (pH 9.5; 1 M) was then added, followed by 0.25 mL of 2 M NaOH (to neutralize the acid). Finally, 200 μL of aqueous $AgNO_3$ (33%, w/v) was added. The analyte was then extracted with a 4 mL solution of $CHCl_3$:methanol (75:25). The mixture was briefly vortexed (20–30 s) and centrifuged (500 × *g*, 5 min) to separate the aqueous and organic layers. The organic phase, containing the analyte, was removed with a syringe, filtered through a PTFE 0.2-μm syringe filter (Whatman Inc., Clifton, NJ) and dried under N_2. The isolated material was reconstituted with 100% methanol (0.1 mL) and mobile phase (0.9 mL). A sample consisting of 50 μL of each solution was then injected onto the HPLC column.

2.9. Determination of unconjugated doxorubicin content (extraction assay)

In another aliquot of the sample (50 μL plasma; 500 μL tissue homogenate), the levels of unconjugated doxorubicin were quantified. Again, a modification of the method described by Seymour et al. (1990) was used. In these studies, the samples were exposed to basic buffer alone (no acid) and processed at ambient temperature, thus permitting only the extraction of unconjugated doxorubicin. To each sample (containing I.S.), 0.5 mL of Tris–HCl buffer (pH 9.5; 1 M) was added. Following a brief vortexing, 200 μL of aqueous $AgNO_3$ (33%, w/v) was added and the unconjugated doxorubicin extracted with 4 mL of $CHCl_3$:methanol (75:25). Following the addition of the organic phase each vial was briefly (20–30 s) vortexed and centrifuged (500 × *g*, 5 min) to separate the aqueous and organic layers. The organic phase was removed and processed as described above.

3. Results

The plasma levels of doxorubicin were determined following a single injection of RGD-targeted doxorubicin-loaded NP (12.5 mg/kg dox equiv.) in female Balb/c mice bearing Cl-66 mammary tumors. The resulting plasma levels over 24 h are shown in Fig. 1 and the PK parameters as determined using

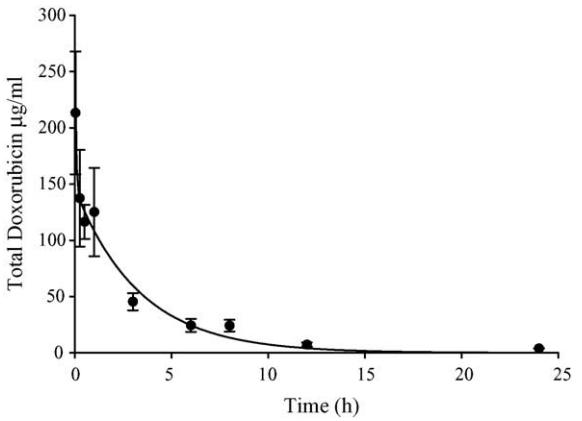

Fig. 1. Pharmacokinetic profile for total doxorubicin content vs. time (up to 24 h), fitted to a bi-exponential model (250 μg doxorubicin equiv. i.v. bolus, mean ± S.D., $n = 5$).

the Kinetica v4.2 program are shown in Table 1. The concentration of total doxorubicin in plasma was 213.3 ± 54.6 μg/mL at 2 min following injection and decreased bi-exponentially to essentially undetectable levels after the 24 h sample (Fig. 1; limit of detection (LOD) = 1 μg/mL). The level of unconjugated doxorubicin at 2 min was 15.4 ± 7.0 μg/mL and was below the LOD after the 15 min sample (1.0 ± 0.9 μg/mL at 15 min). The PK profile of total doxorubicin in plasma samples from 2 min to 24 h fitted a bi-exponential model (Fig. 1; $R^2 = 0.9964$). The terminal elimination half-life was determined to be 5.99 h (Table 1). This contrasts with elimination half-life of 7.3 h for doxorubicin in saline (Gustafson et al., 2002). Doxorubicin formulated in NPs had a clearance of 0.422 mL h^{-1}.

The distribution of doxorubicin into tumors was determined at five time points: 0.25, 6, 24, 48 and 120 h. Twenty-four hours following injection of the RGD-NP formulation (ca. 12.5 mg/kg doxorubicin equiv.) the amount of total drug detected was 17.9 ± 5.8 μg drug/g

Table 1
Pharmacokinetic parameters for total doxorubicin concentration in plasma (i.v. dose = 250 μg)

Parameter	Value
C_{max} (μg/mL)	213.3
T_{max} (h)	0.0333
Terminal half-life ($t_{1/2\beta}$) (h)	5.99
Area under curve (AUC) (μg h mL^{-1})	593
Volume of distribution (V_{ss}) (mL)	2.63
Clearance (Cl) (mL × h^{-1})	0.422

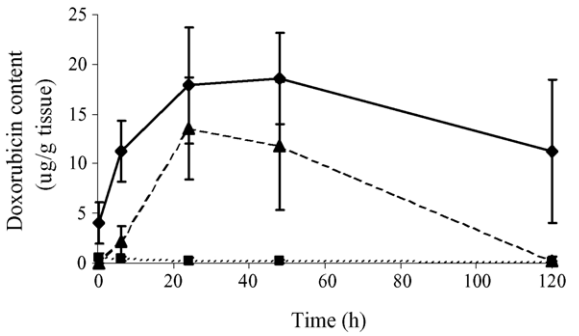

Fig. 2. Plot of total (♦) and free (■) doxorubicin content and metabolite of doxorubicin (▲) in tumor, expressed as μg drug/g tissue (mean ± S.D., $n = 5$).

of tumor tissue (Fig. 2), which was equal to 2.1% of the administered dose. The levels of doxorubicin in the tumors increased steadily until 48 h, at which time the total doxorubicin concentration remained relatively stable with 11.3 ± 7.2 μg/g (1.5% of dose) still present at study completion (120 h). Low levels of unconjugated doxorubicin were observed with the highest level at 15 min (0.51 μg/g tumor). A substantial amount of a metabolite that was likely to be either doxorubicinol or doxorubicinone was also found in tumor. Unfortunately, using these chromatographic conditions, doxorubicinol and doxorubicinone had the same retention time (4.3 min). Whilst no metabolite was detected in the 15 min samples, the concentration subsequently increased with time. At 24 h, the mean concentration of metabolite(s) peaked, reaching 1.6% of administered dose as compared to 2.1% of total doxorubicin. This metabolite was neither observed in any other tissue nor in plasma.

The distribution of doxorubicin in solid organs (Figs. 3 and 4) was determined at the same five time points as the tumors (0.25, 6, 24, 48 and 120 h). As with the doxorubicin levels in the tumors, the doxorubicin content in the liver and spleen accumulated with time (Fig. 3). Of all the organs, the liver contained the highest level of total doxorubicin, reaching 144.8 ± 10.9 μg/g tissue at 48 h or 56% of the doxorubicin injected at time 0. The unconjugated doxorubicin content in the liver was relatively low, being 3.1 ± 0.6 μg/g tissue (Fig. 3) at the same time point (1.2% of dose). The C_{max} of unconjugated doxorubicin in the liver was 15.2 μg/g tissue (6.8% of dose) at $t = 15$ min. The highest level found in the spleen was 106.7 ± 26.0 μg/g tissue, also

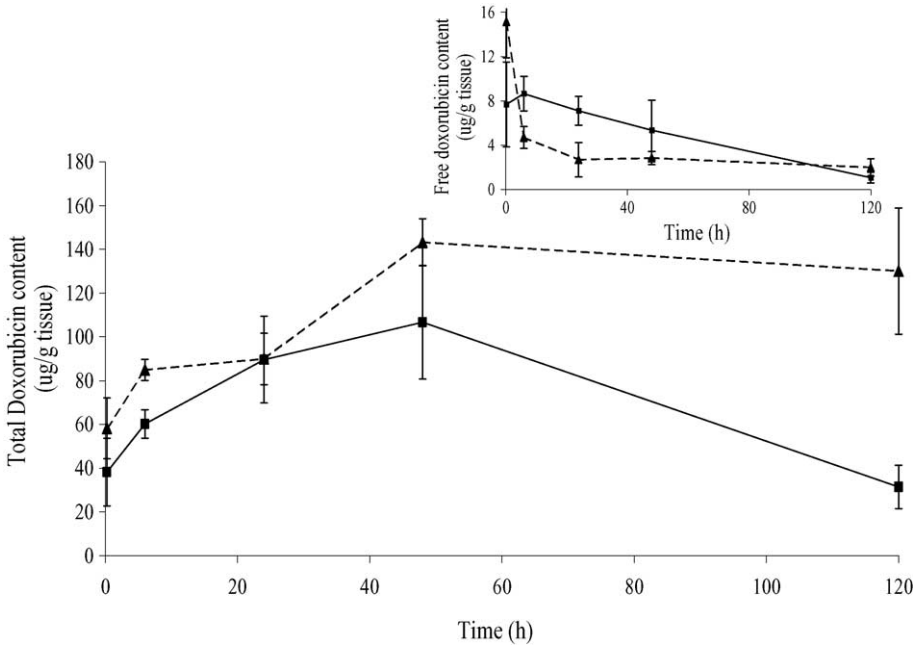

Fig. 3. Plots of total and free doxorubicin content in liver (▲) and spleen (■), expressed as μg drug/g tissue (mean ± S.D., $n = 5$).

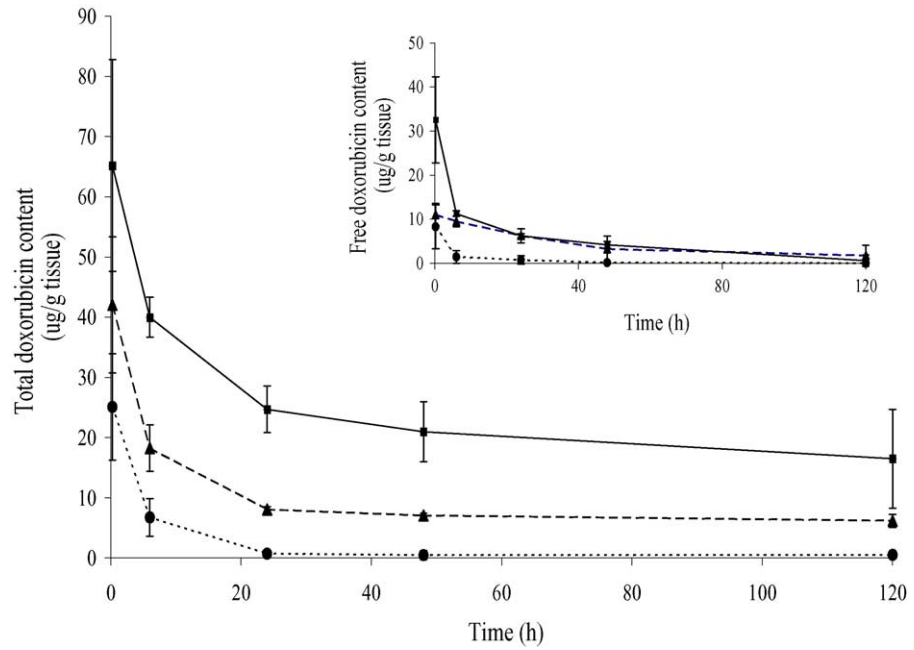

Fig. 4. Plots of total and free doxorubicin content in lung (▲), heart (●) and kidney (■), expressed as μg drug/g tissue (mean ± S.D., $n = 5$).

at 48 h. However, due to a smaller organ weight (ca. 100–150 mg), the total doxorubicin in the mouse spleen at 48 h is equal to less than 3.5% of the administered dose.

In contrast to the increasing levels of doxorubicin in the tumor, liver and spleen, the concentrations of doxorubicin in the heart, lungs and kidneys decreased more rapidly with time (Fig. 4). At 15 min following the i.v. injection of the NP formulation, 2.6, 0.8 and 6.1% of the doxorubicin injected was found in the lungs, heart and kidneys, respectively. The unconjugated doxorubicin content in the various tissues is also illustrated in Figs. 3 and 4 (inset). In all cases, free drug content was lower than total drug content, indicating that large amounts of the injected drug were still bound to the NPs (tumor being the exception due to the formation of a metabolite). Biodistribution to the kidneys (Fig. 4) was higher than that found in the tumor; however, no accumulation of drug was evident. The total doxorubicin level decreased from a high of 65.2 ± 17.6 μg/g tissue at 15 min (6.1% of the administered dose) to 24.7 ± 3.9 μg/g tissue (2.5% of dose) at 24 h, and continued to decrease for the remainder of the study. The renal 15-min sample time point also showed a high level of unconjugated doxorubicin: 32.6 ± 9.8 μg/g tissue. Cardiomyopathy is a unique characteristic of anthracycline antibiotics such as doxorubicin (Martindale, 1996) and one goal of NP formulation was to reduce exposure of the heart to the drug. This was achieved with a C_{max} of 25.1 ± 8.8 μg/g cardiac tissue at 15 min (Fig. 4), representing only 0.8% of the administered dose. Further, the mean drug level in the heart decreased to 6.7 μg/g tissue (0.24% of dose) by 6 h and was <0.7 μg/g tissue (<0.03% of dose) at 24 h, where it remained for the remainder of the study. In the lungs, the total doxorubicin level was highest at 15 min (C_{max}: 42.0 ± 11.3 μg/g tissue, representing 2.6% of administered dose; Fig. 4) but, as with the heart, no accumulation of drug was evident. At $t = 24$ h, total doxorubicin content fell to 8.1 ± 0.5 μg/g pulmonary tissue (0.4% of dose).

The relationship between drug concentrations in plasma and tissues is illustrated in Fig. 5 by a comparison of tissue to plasma ratios for total doxorubicin content. The ratio for all tissues was low at $t = 15$ min, reflecting the high concentration of drug in plasma immediately following i.v. administration of the dose. The ratio increased with time as drug

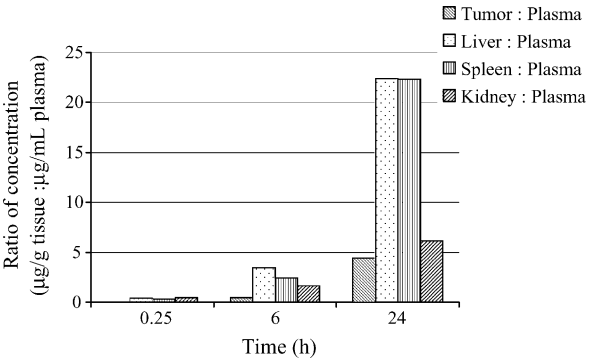

Fig. 5. Ratio of total doxorubicin for selected tissues:plasma ((μg/g)/(μg/mL)) at 0.25, 6 and 24 h (mean, $n = 5$).

accumulated in the tissues and the plasma concentration exponentially decreased. At $t = 24$ h, the concentration ratio was highest in liver and spleen (22.4 and 22.3 (μg/g)/(μg/mL), respectively), followed by kidney and tumor (6.1 and 4.4 (μg/g)/(μg/mL), respectively). The AUC $_{(0–T)}$ for the various tissues was calculated using the trapezoidal rule ((0–T) = 0–∞ plasma; 0–120 h tissues). These studies revealed an AUC of 593 μg h mL^{-1} for plasma, 8966 μg h mL^{-1} for the spleen, 14,630 μg h mL^{-1} for the liver, 211 μg h mL^{-1} for cardiac tissue, 1073 μg h mL^{-1} for pulmonary tissue, 2790 μg h mL^{-1} for renal tissue and 1815 μg h mL^{-1} for tumor tissue. This quantifies the extent of tissue exposure to doxorubicin, suggesting a limited potential for cardiac damage and increased tumor exposure similar to the kidneys and greater than the lungs, but substantially less than that found with the spleen and liver. Further, it should be noted that this is the AUC for 0–120 h, which in the case of the liver and tumor underestimates the exposure.

4. Discussion

Covalent linkage of doxorubicin to NPs with an IMMA core and i.v. injection (ca. 12.5 mg/kg) resulted in a bi-exponential PK profile. The plasma concentration profile compares favorably with that reported by Seymour et al. (1990). In those studies, the PK of a doxorubicin-HPMA conjugate was studied following i.v. administration of the conjugate at a 5 mg/kg doxorubicin equivalent dose. At 30 min post-injection, Seymour et al. (1990) reported the total drug concentra-

tion in plasma to be approximately 40 μg/mL. This is consistent with the plasma concentration of 116 μg/mL (total drug; $t = 30$ min) observed in our studies, after accounting for the 2.5-fold higher dose. Comparisons at later times are limited, as Seymour et al. did not sample plasma levels between 1 and 24 h post-injection.

The PK of *free* doxorubicin has been studied in a number of species, including rodents and humans. Typically, after i.v. administration, blood levels fall rapidly as the drug is distributed to various tissues. A slow elimination is then seen. Following a 10 mg/kg i.v. bolus administration of free drug to healthy Balb/c mice, Gustafson et al. (2002) analyzed doxorubicin plasma concentrations for at least 8 h post-dose. They reported the $t_{1/2}\alpha$ and $t_{1/2}\beta$ of doxorubicin to be 4.0 min and 7.3 h, respectively.

Whilst the plasma $t_{1/2}\beta$ of our formulation is similar to that for free drug as determined by Gustafson et al. (2002), our studies were in tumor-bearing mice, which may impact the PK and appears to have resulted in drug metabolism within the tumor. Thus, removal of the NP formulation from the circulation to the tissues (including the tumor) may be altered compared to healthy animals. Importantly, a further prolongation of the NPs circulation in plasma may be possible through modification of the particle surface (i.e., the amount and type of PEGylation).

As stated earlier, up to 2.1% of the administered dose was detected in the tumor. Whilst relatively low, the drug tended to accumulate in sufficient quantity to exert a chemotherapeutic effect on this tissue (data not shown). The optimization of effective targeting ligand(s) will likely lead to an increase in drug concentration within the tumor. Unfortunately, the in vivo analysis of RGD was beyond the scope of this study. Further effort will be required to assess the in vivo efficacy of RGD or other ligands, their optimal concentration and orientation on the particle surface.

Importantly, a majority of the doxorubicin in the tumor was found as a metabolite. This metabolite formation, unique to tumor samples, may be attributed to the lowered pH of tumors and/or an altered metabolic state in this tissue (Tannock and Rotin, 1989; Griffiths, 1991). The presence of the metabolite is encouraging from a therapeutic standpoint as it suggests tumor specific degradation of the NPs and subsequent release of active drug into the tumors. Clearly, more studies would be required to define the mechanism of this tumor-specific metabolism. One question raised by these studies was the lability of the amide bond linking the doxorubicin to the particle matrix. The linkage between drug and NP must be stable in the bloodstream yet capable of hydrolysis upon entering the lysosome of the tumor cell. With regards to doxorubicin-HPMA, peptidic spacers have been used to achieve a selected lysosomal cleavage (Kopeček et al., 2000). The presence of a metabolite in the tumor samples may indicate some degree of lability for our NPs, although the metabolite may be explained by the metabolism of the free drug component.

The liver contained the highest level of total doxorubicin, reaching 144.8 ± 10.9 μg/g tissue at $t = 48$ h (Fig. 3). However, the unconjugated doxorubicin content in the liver was relatively low, being 3.1 ± 0.6 μg/g tissue at the same time point. The low amount of unconjugated doxorubicin detected in the liver and an absence of any known metabolites (e.g., doxorubicinol and doxorubicinone) suggested a low metabolic activity with respect to the test article. That is, the conjugated doxorubicin NPs were heavily distributed to the liver but appeared to be largely isolated/stored in this organ over the 5-day study. Kuiper et al. (1994) reported that particles exposing a galactose moiety were taken up and isolated by hepatic Kupffer cells of the rat. Our particles, largely composed of another carbohydrate, the inulin derivative IMMA, may share a similar targeted distribution.

Total doxorubicin content in the spleen (Fig. 3) was also relatively high, yet as with the liver, unconjugated doxorubicin extracted from the spleen was relatively low (<0.2% of the administered dose after 48 h). Again, the test article appeared to be taken up into the tissue, but remained to a large extent conjugated to the NP. The RES effect may contribute to the high ratios of concentration (tissue:plasma) for liver and spleen (Fig. 5) and may be due, in part, to the particulate nature of the NPs. However, a detailed microscopic study would be required to confirm this hypothesis.

The biodistribution studies of the drug to the kidneys (Fig. 4) revealed a high initial concentration, although no accumulation occurred. Further, of the total doxorubicin detected at 15 min in the kidney, almost half was present in its *free form*, perhaps reflecting renal excretion. It should also be noted that the NPs are large enough to avoid glomerular filtration. In contrast to the kidneys, minimal cardiac distribution of doxorubicin

was observed and negligible amounts were present as free drug.

The RGD-targeted NP described in this report is one of a number of formulations that our laboratory is currently testing. It is our intention to increase drug-NP uptake by the tumor, tumor cells and tumor cell vasculature, and minimize NP distribution to the liver and spleen. This will be attempted in part by increasing the molecular weight attachment density of PEG chains, and through the selection of targeting ligands. While an increase in circulation time with an increase in PEG molecular weight is readily predictable, tissue distribution and cellular uptake are contradictory and likely depend on issues specific to a particular PEGylated structure. For example, the PEGylation of liposomes expectedly led to an increase in circulation time, but did not lead to increase tumor accumulation or efficacy (Hong et al., 1999).

5. Conclusions

In summary, the PK and biodistribution of doxorubicin administered in a carbohydrate NP formulation was determined in plasma, tumor and five selected tissues using a Cl-66-tumor-bearing mouse model. The PK of doxorubicin (total drug content) in plasma followed a two-compartment model following i.v. (bolus) administration of the NPs. The terminal half-life was determined to 5.99 h.

The accumulation of doxorubicin was high in both the liver and spleen. Notably, unconjugated doxorubicin (and doxorubicin metabolites such as doxorubicinol) content was low in the liver, suggesting that upon distribution to this organ, the NPs are not readily metabolized. Exposure of doxorubicin to cardiac tissue was low.

Finally, following administration, drug accumulated in the tumor, reaching 2.1% of the administered dose at $t = 24$ h. A metabolite—suspected to be doxorubicinol or doxorubicinone—was also observed in these tumor samples. This metabolite was not seen in any other tissue and may be attributed to enzymatic activity, a decreased pH or an otherwise altered metabolic state in the tumor. The presence of a metabolite in this tissue alone is indicative of a 'tumor-specific' drug-nanoparticle lability, and may present a therapeutic advantage.

Acknowledgments

The work was supported by a contract from the National Cancer Institute. The authors wish to thank Sowmya Chollate for assistance in PK sample preparation and analysis, and Amy Hsu, Almita Heramia, Anthony Lam and Andrew Goodwin for nanoparticle fabrication.

References

Devita, V., Hellman, S., Rosenberg, S., 1989. Cancer, Principles and Practice of Oncology, third ed. Lippincott, Philadelphia, 376 pp.

Dexter, D.L., Kowalski, H.M., Blazar, B.A., Fligiel, Z., Vogel, R., Heppner, G.H., 1978. Heterogeneity of tumor cells from a single mouse mammary tumor. Cancer Res. 38, 3174–3181.

Duncan, R., Coatsworth, J.K., Burtles, S., 1998. Preclinical toxicology of a novel polymeric antitumour agent: HPMA copolymer-doxorubicin (PK1). Hum. Exp. Toxicol. 17, 93–104.

Griffiths, J.R., 1991. Are cancer cells acidic? Br. J. Cancer 64, 425–427.

Gustafson, D.L., Rastatter, J.C., Colombo, T., Long, M.E., 2002. Doxorubicin pharmacokinetics: macromolecule binding, metabolism, and excretion in the context of a physiologic model. J. Pharm. Sci. 91, 1488–1501.

Harris, L., Batist, G., Belt, R., Rovira, D., Navari, R., Azarnia, N., Welles, L., Winer, E., 2002. Liposome-encapsulated doxorubicin compared with conventional doxorubicin in a randomized multicenter trial as first-line therapy of metastatic breast carcinoma. Cancer 94, 25–36.

Hong, R.L., Huang, C.J., Tseng, Y.L., Pang, V.F., Chen, S.T., Liu, J.J., Chang, F.H., 1999. Direct comparison of liposomal doxorubicin with or without polyethylene glycol coating in C-26 tumor-bearing mice: is surface coating with polyethylene glycol beneficial? Clin. Cancer Res. 5, 3645–3652.

Kopeček, J., Kopečková, P., Minko, T., Lu, Z.-R., 2000. HPMA copolymer-anticancer drug conjugates: design, activity, and mechanism of action. Eur. J. Pharm. Biopharm. 50, 61–81 (review).

Kovar, M., Mrkvan, T., Strohalm, J., Etrych, T., Ulbrich, K., Stastny, M., Rihova, B., 2003. HPMA copolymer-bound doxorubicin targeted to tumor-specific antigen of BCL1 mouse B cell leukemia. J. Control Release 92, 315–330.

Kuiper, J., Bakkeren, H.F., Bissen, E.A.L., Van Berkel, T.J.C., 1994. Characterization of the interaction of galactose-exposing particles with rat kupffer cells. Biochem. J. 299, 285–290.

Kwon, G.S., 2003. Polymeric micelles for delivery of poorly water soluble compounds. Crit. Rev. Ther. Drug Carrier Syst. 20, 357–403.

Kwon, G., Suwa, S., Yokoyama, M., Okano, T., Sakurai, Y., Kataoka, K., 1994. Enhanced tumor accumulation and prolonged circulation times of micelle-forming poly(ethylene oxide-aspartate) block copolymer–adriamycin conjugates. J. Control Release 29, 17–23.

Martindale, 1996. Royal Pharmaceutical Society London, 31st ed. Pharmaceutical Press, London, 567 pp.

Miller, F.R., Miller, B.E., Heppner, G.H., 1983. Characterization of metastatic heterogeneity among subpopulations of a single mouse mammary tumor: heterogeneity in phenotypic stability. Invasion Metastasis 3, 22–31.

Pasqualini, R., Koivunen, E., Ruoslahti, E., 1997. Alpha v integrins as receptors for tumor targeting by circulating ligands. Nat. Biotechnol. 15, 542–546.

Schiffelers, R.M., Koning, G.A., ten Hagen, T.L., Fens, M.H., Schraa, A.J., Janssen, A.P., Kok, R.J., Molema, G., Storm, G., 2003. Antitumor efficacy of tumor vasculature-targeted liposomal doxorubicin. J. Control Release 91, 115–122.

Seymour, L.W., Ulbrich, K., Strohalm, J., Kopeček, J., Duncan, R., 1990. The pharmacokinetics of polymer-bound adriamycin. Biochem. Pharmacol. 39, 1125–1131.

Talmadge, J.E., Fidler, I.J., Oldham, R.K., 1985. Screening for biological response modifiers: methods and rationale. Martinus Nijhoff, The Hague.

Tannock, I.F., Rotin, D., 1989. Acid pH in tumors and its potential for therapeutic exploitation. Cancer Res. 49, 4373–4384.

Ulbrich, K., Etrych, T., Chytil, P., Jelinkova, M., Rihova, B., 2003. HPMA copolymers with pH-controlled release of doxorubicin: in vitro cytotoxicity and in vivo antitumor activity. J. Control Release 87, 33–47.

Van Asperen, J., Van Tellingen, O., Beijnen, J.H., 1998. Determination of doxorubicin and metabolites in murine specimens by high-performance liquid chromatography. J. Chromatog. B 712, 129–143.

Vermorken, J.B., 2003. The role of anthracyclines in second-line therapy of ovarian cancer. Int. J. Gynecol. Cancer 13 (Suppl. 2), 178–184.

Von Hoff, D.D., Layard, M.W., Basa, P., Davis Jr., H.L., Von Hoff, A.L., Rozencweig, M., Muggia, F.M., 1979. Risk factors for doxorubicin-induced congestive heart failure. Ann. Intern. Med. 91, 710–717.